Confounding effects of oxygen and temperature on the TEX_{86} signature of marine Thaumarchaeota

Wei Qin[a], Laura T. Carlson[b], E. Virginia Armbrust[b], Allan H. Devol[b], James W. Moffett[c], David A. Stahl[a,1], and Anitra E. Ingalls[b,1]

[a]Department of Civil and Environmental Engineering, University of Washington, Seattle, WA 98195; [b]School of Oceanography, University of Washington, Seattle, WA 98195; and [c]Department of Biological Sciences, University of Southern California, Los Angeles, CA 90089

Edited by Donald E. Canfield, Institute of Biology and Nordic Center for Earth Evolution, University of Southern Denmark, Odense M., Denmark, and approved July 31, 2015 (received for review January 23, 2015)

Marine ammonia-oxidizing archaea (AOA) are among the most abundant of marine microorganisms, spanning nearly the entire water column of diverse oceanic provinces. Historical patterns of abundance are preserved in sediments in the form of their distinctive glycerol dibiphytanyl glycerol tetraether (GDGT) membrane lipids. The correlation between the composition of GDGTs in surface sediment and the overlying annual average sea surface temperature forms the basis for a paleotemperature proxy (TEX_{86}) that is used to reconstruct surface ocean temperature as far back as the Middle Jurassic. However, mounting evidence suggests that factors other than temperature could also play an important role in determining GDGT distributions. We here use a study set of four marine AOA isolates to demonstrate that these closely related strains generate different TEX_{86}–temperature relationships and that oxygen (O_2) concentration is at least as important as temperature in controlling TEX_{86} values in culture. All of the four strains characterized showed a unique membrane compositional response to temperature, with TEX_{86}-inferred temperatures varying as much as 12 °C from the incubation temperatures. In addition, both linear and nonlinear TEX_{86}–temperature relationships were characteristic of individual strains. Increasing relative abundance of GDGT-2 and GDGT-3 with increasing O_2 limitation, at the expense of GDGT-1, led to significant elevations in TEX_{86}-derived temperature. Although the adaptive significance of GDGT compositional changes in response to both temperature and O_2 is unclear, this observation necessitates a reassessment of archaeal lipid-based paleotemperature proxies, particularly in records that span low-oxygen events or underlie oxygen minimum zones.

TEX_{86} | oxygen | temperature | Thaumarchaeota | GDGT

Marine ammonia-oxidizing archaea (AOA) (now assigned to the phylum Thaumarchaeota) are among the most ubiquitous and abundant organisms in the ocean, constituting up to 40% of microbial plankton in the meso- and bathypelagic zones (1–4). They are generally recognized as the main drivers of oceanic nitrification (5–7), are closely coupled with anammox organisms in oxygen minimum zones (OMZs) (8–10), and have been implicated as a source of the greater part of oceanic emissions of the ozone-depleting greenhouse gas nitrous oxide (11). Their wide habitat range suggests both high ecotypic diversity and adaptive capacity (12, 13).

The adaptive basis for their dominant role in the nitrogen cycle has in part been attributed to highly efficient systems of ammonia oxidation and carbon fixation, and a primarily copper-based respiratory system that reduces reliance on iron availability in the often iron-depleted marine environment (13–16). In addition, compositional regulation of their distinctive glycerol dibiphytanyl glycerol tetraether (GDGT) lipid membrane (*SI Appendix*, Fig. S1) is implicated in adaptation and acclimation to energy-limited environments (17). Relative to the bacterial membrane bilayer, the membrane-spanning lipids of archaea are less permeable to ions and protons (18, 19). Lower permeability is suggested to reduce maintenance energy costs, an important adaptive feature of extreme oligophiles such as the AOA. Thus, growth temperature-dependent modulation of membrane composition is likely associated with maintenance of appropriate permeability, as well as other membrane functions (18).

The influence of temperature on membrane composition has been the major focus of studies of the environmental distribution of archaeal membrane lipids in the present and for interpreting lipids preserved in the sedimentary record (20). In particular, the correlation between sea surface temperature (SST) and the cyclopentane ring distribution of GDGTs in a sample set of globally distributed core top sediments is the basis for a widely applied paleotemperature proxy, TEX_{86} (TetraEther indeX of lipids with 86 carbon atoms). The TEX_{86} proxy has been used to reconstruct surface ocean temperature as far back as the Middle Jurassic (21, 22). However, the extent to which temperature is the causative agent behind the correlation has not fully been examined. Moreover, it is not evident how a group of organisms that live at depths below the upper-photic zone and are the dominant prokaryote of the abyss can record SST via a physiological response.

Interpretation of TEX_{86} records that deviate from expectation are usually interpreted from the point of view that temperature is still the main underlying influence on TEX_{86}. That is, disagreement with other proxy records, unreasonably large swings in TEX_{86} over short time periods, or warm biases in semienclosed basins (Mediterranean and Red Sea) have been attributed to changes in circulation, seasonal timing of production, selective export to sediments, or to autochthonous archaeal populations having slightly different temperature responses (20, 23–25). Large

Significance

Ammonia-oxidizing archaea (AOA) are among the most abundant microorganisms in the ocean. Apart from having a major influence on the nitrogen cycle, the glycerol dibiphytanyl glycerol tetraether (GDGT) membrane lipids of AOA are widely used to reconstruct past sea surface temperatures. We here provide compelling evidence that the composition of membrane lipids of marine AOA show strain-specific dependence on temperature. We also show that oxygen (O_2) concentration greatly influences membrane lipid composition, leading to significant increases in TEX_{86}-derived temperatures with increasing O_2 limitation. This finding challenges the convention that GDGT composition correlates solely with ocean temperature and necessitates a reassessment of archaeal lipid-based paleoclimate proxies, particularly when applied to environments where O_2 is depleted.

Author contributions: W.Q., D.A.S., and A.E.I. designed research; W.Q. and L.T.C. performed research; W.Q., L.T.C., D.A.S., and A.E.I. analyzed data; and W.Q., L.T.C., E.V.A., A.H.D., J.W.M., D.A.S., and A.E.I. wrote the paper.

The authors declare no conflict of interest.

This article is a PNAS Direct Submission.

[1]To whom correspondence may be addressed. Email: dastahl@u.washington.edu or aingalls@uw.edu.

This article contains supporting information online at www.pnas.org/lookup/suppl/doi:10.1073/pnas.1501568112/-/DCSupplemental.

discrepancies between in situ and TEX_{86}-derived temperatures from suspended particulate matter (SPM) samples, particularly from low-oxygen (O_2) environments, have been observed in many regions (25–28), but O_2 has not explicitly been suggested as a cause of these discrepancies. Instead, it is thought that some local environments select for ecotypes having slightly different TEX_{86}–temperature relationships.

TEX_{86} reconstructions of the distant past, when oceanic conditions could be quite different from today, present the greatest challenge to interpretation. For example, inferred Cretaceous SSTs are higher than physically plausible for the ocean (29). Thus, considerable efforts have been made to develop and apply new TEX_{86} equations suitable for high-temperature environments (TEX_{86}^{H}), low-temperature environments (TEX_{86}^{L}), local systems (TEX_{86}'), the marine water column, and mesocosms (24, 30–33).

The availability of a number of pure cultures of marine AOA (12) now serves to test strain-specific response to temperature, as well as the influence of ecophysiological factors other than temperature, on lipid composition. Here we grew pure cultures of four marine AOA strains to evaluate the influence of growth conditions on core lipid composition. Despite relatively close phylogenetic relationships, these isolates are physiologically distinct ecotypes recovered from dimly lit deep waters, the nitrite maximum near the euphotic zone, and near-surface sediment (12). The influence of temperature and dissolved O_2 (DO) on GDGT composition and TEX_{86} values was examined by independently varying these two important environmental variables. These experiments revealed significant strain-specific variation in temperature-associated GDGT distribution. More striking was the observation that in addition to temperature, the DO concentration had a profound impact on membrane composition, skewing TEX_{86}-derived temperatures by more than 20 °C at a single growth temperature. These findings necessitate reinterpretation and possible reformulation of this important paleoclimate proxy.

Results

Early stationary phase cultures were used to investigate total GDGT content and the distribution of GDGTs in different AOA strains [strains are described in detail in Qin et al. (12)]. Cell pellet hydrolysis ensured the complete recovery of all cellular lipids and removed polar head groups from intact GDGTs so they could be analyzed as core GDGTs (34). Different strains of marine AOA contained variable amounts of total GDGTs per cell (calculated based on cell counts and lipid abundance) and each strain contained a similar amount of total lipids per cell regardless of the growth temperature. Strain HCE1 contained 1.47 ± 0.096 fg GDGTs per cell (at 15–20 °C, $n = 6$), which was less than half of the total GDGTs recovered from PS0 cells (3.01 ± 0.065 fg per cell at 25 °C, $n = 3$) (*SI Appendix*, Table S1). Cells of strains HCA1 and SCM1 contained similar lipid content (2.04 ± 0.21 fg per cell at 15–30 °C for HCA1, $n = 12$ and 2.08 ± 0.12 fg per cell at 20–30 °C for SCM1, $n = 9$; *SI Appendix*, Table S1). These values were within the range reported for the cellular lipid contents of SCM1 and natural marine communities dominated by AOA (0.1–8.5 fg per cell) (17, 35). GDGTs of SCM1 accounted for ∼10% of dry cell weight (20 fg per cell) (13). This value is at the higher end of previous estimates for methanogenic and thermoacidophilic archaea that contain 2.5–10% total lipids on a dry weight basis (36–38).

All isolates showed substantially different TEX_{86} values when grown at 25 °C (0.56 ± 0.02 for HCA1, 0.51 ± 0.01 for SCM1, 0.42 ± 0.01 for HCE1, and 0.38 ± 0.01 for PS0) (*SI Appendix*, Table S1). TEX_{86} values calculated using the calibration curve of Kim et al. (39) correspond to TEX_{86}-derived temperatures ranging from 10.5 to 20.7 °C, all below their actual growth temperature of 25 °C (Fig. 1). To further test the strain-specific relationship between TEX_{86} values and growth temperatures, SCM1 (optimum growth temperature at 32 °C), HCA1, and HCE1 (optimum growth temperatures at 25 °C) were incubated at temperatures ranging from 15 to 35 °C, 10–30 °C and 10–25 °C, respectively (see *SI Appendix*, Fig. S2 and Table S1 for experimental details and results at different growth temperatures). The relationship between TEX_{86} values and growth temperatures of SCM1 was a linear function, showing a general pattern of increased TEX_{86} values with increasing temperature (*SI Appendix*, Fig. S3*A*; see *SI Appendix*, Fig. S4*A* and Table S2 for additional details of relative abundance of GDGTs):

$$TEX_{86} = 0.015T + 0.21 \left(r^2 = 0.85\right). \quad [1]$$

A linear relationship was also found between the TEX_{86}-derived temperature reconstructed using the Kim et al. (39) calibration equation and actual growth temperature of SCM1 (Fig. 2*A*). These calculated TEX_{86} temperatures were 0.13–7.28 °C lower than incubation temperatures, explaining the difference between the global calibration line ($T = -10.78 + 56.2 \times TEX_{86}$) and the culture correlation line ($T = -14 + 66.7 \times TEX_{86}$). In contrast, there was no linear dependence of growth temperature on the TEX_{86} value of strains HCA1 and HCE1. Instead, the data of HCA1 (Eq. **2**) and HCE1 (Eq. **3**) fitted best to polynomial curves, reaching the maximum TEX_{86} values at 20 °C (*SI Appendix*, Fig. S3 *B* and *C*; see *SI Appendix*, Fig. S4 *B* and *C* and Table S2 for additional details of relative abundance of GDGTs):

$$TEX_{86} = -0.0006T^2 + 0.023T + 0.33 \left(r^2 = 0.94\right) \quad [2]$$

$$TEX_{86} = -0.0017T^2 + 0.054T + 0.11 \left(r^2 = 0.89\right). \quad [3]$$

Similarly, second-order polynomials resulted in good fits to TEX_{86}-derived temperatures of HCA1 and HCE1 vs. incubation temperature (Fig. 2 *B* and *C*). The temperatures derived from TEX_{86} values of HCA1 and HCE1 reflected the in situ temperatures, within calibration error, at 20 °C (TEX_{86} temperatures of HCA1 and HCE1 were 21.1 °C and 19.3 °C, respectively). However, large discrepancies between TEX_{86}-derived temperatures and actual growth temperatures (up to 12 °C) were observed at low- and high-growth temperatures of HCA1 and HCE1. All isolates had different ring index values (a common metric of GDGT cyclization) when grown at 25 °C (*SI Appendix*, Table S2) (40). The ring index values of strains SCM1, HCA1, and HCE1 all showed a linear increase in cyclization of total GDGTs with increasing temperature (Fig. 3).

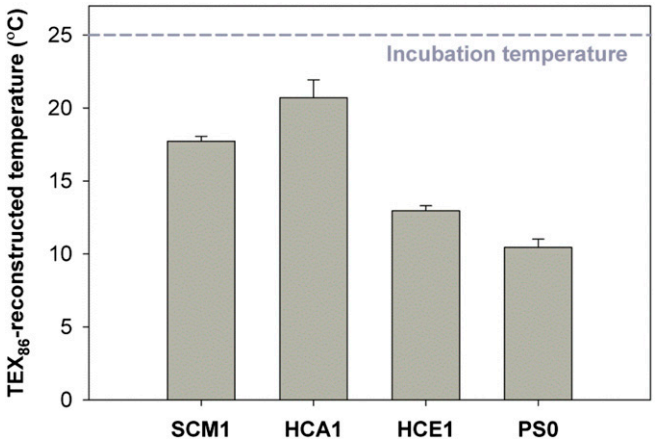

Fig. 1. Reconstructed TEX_{86}-derived temperatures of four marine AOA isolates incubated at 25 °C (dashed line). Each bar represents the average of measurements from triplicate incubations and at least duplicate injections. Error bars are the SD among average values of triplicate incubations.

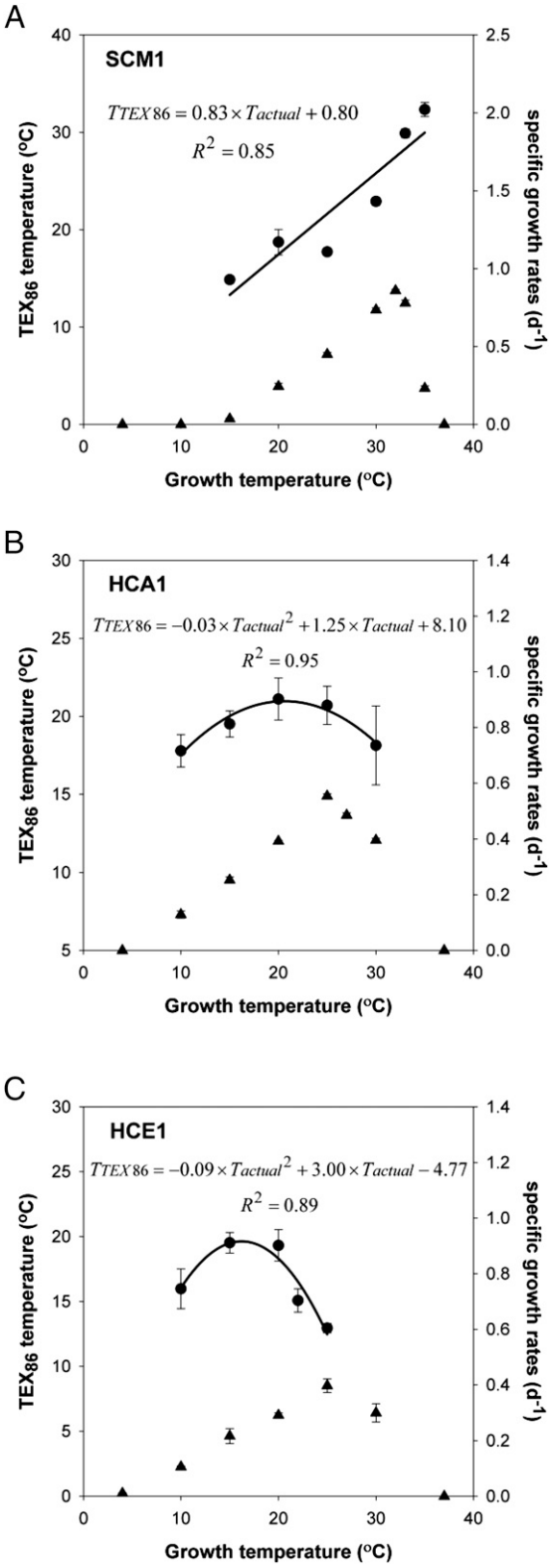

Fig. 2. Correlation of TEX_{86}-derived temperature (filled circles) with growth temperature of strains SCM1 (*A*), HCA1 (*B*), and HCE1 (*C*). Filled triangles represent the temperature dependence of the growth of strains SCM1 (*A*), HCA1 (*B*), and HCE1 (*C*) (in terms of specific growth rates per day). All plotted data represent the average of measurements from triplicate incubations. Error bars represent the SD of triplicates.

In addition to the expected adaptation to changes in temperature, the observation of abundant and transcriptionally active AOA populations near the oxic–anoxic boundary of OMZs also suggested a capacity to grow in highly O_2-depleted waters (9, 41). Both SCM1 and PS0 were shown to be capable of growing at very low O_2 (0.1–21% of initial headspace O_2 in sealed culture bottles; see *SI Appendix*, Fig. S5 and Table S3 for experimental details and results at different percentages of O_2). All ammonia (10 μmol) was completely oxidized to nitrite when O_2 was in stoichiometric excess (0.5–21% initial headspace O_2). In accordance with the established reaction stoichiometry of 1 mol NH_3 oxidized per 1.5 mol O_2 consumed (13), ∼15–1,238 μmol of O_2 remained at the end of the incubation (*SI Appendix*, Fig. S5 and Table S3). In contrast, all headspace O_2 was consumed at 0.1% and 0.2% initial O_2, resulting in residual ammonia and a lower level of nitrite production (∼5.1 and ∼8.2 μmol nitrite, respectively), also consistent with predicted reaction stoichiometry (∼4.0 and ∼7.8 μmol nitrite for 0.1% and 0.2% O_2, respectively) (*SI Appendix*, Fig. S5 and Table S3). Ammonia oxidation was coupled to growth at all O_2 concentrations. The cell densities of early stationary phase cultures of SCM1 and PS0 were 13–27 times and 25–29 times higher than initial cell densities, respectively (*SI Appendix*, Table S3).

Because marine AOA demonstrate the ability to grow at very low O_2 in the laboratory and the environment, we next asked whether changes in membrane composition might also be associated with the growth of AOA at low O_2 concentrations. The relative abundances of GDGT-2 and GDGT-3 (*SI Appendix*, Figs. S1 and S6) increased as initial headspace O_2 concentration decreased (*SI Appendix*, Fig. S7 and Table S4). Notably, the abundance of GDGT-2 in SCM1 and PS0 showed a significant and continuous increase from 12.4% and 7.7% at 21% O_2 to 16.6% and 27.0% at 0.1% O_2, respectively. In contrast, a 5.2% and 5.7% decrease in the relative abundance of GDGT-1 was observed between 21% O_2 and 0.1% O_2 treatments for SCM1 and PS0, respectively (*SI Appendix*, Fig. S7 and Table S4). These changes along with changes in GDGT-0 and crenarchaeol abundance were reflected in the increase in ring index values as the O_2 concentration decreased with the exception of the lowest O_2 treatments (*SI Appendix*, Table S4). Crenarchaeol regioisomer (cren′) (*SI Appendix*, Fig. S1) was detected in low abundance (<1.3%) in all samples. The relative decrease in GDGT-1, and increase in GDGT-2 and GDGT-3, at low O_2 concentrations resulted in higher calculated TEX_{86} temperatures in O_2-deficient cultures. Nearly 12 °C of TEX_{86}-derived temperature elevation reconstructed using the Kim et al. (39) calibration equation was observed for strain SCM1 from 21% O_2 to 0.1% O_2 (Fig. 4*A*). Likewise, the TEX_{86}-derived temperatures of PS0 were 11.4 °C below incubation temperature (26 °C) at 21% O_2, but changed to 9.9 °C above incubation temperature at 0.1% O_2 (Fig. 4*B*). Although some change in DO is expected with growth, the comparable growth kinetics observed at the higher, but nonlimiting, O_2 concentrations suggest that O_2 concentration primarily influences lipid composition (*SI Appendix*, Fig. S5).

Discussion

Although the TEX_{86} paleothermometer has been applied in diverse depositional settings across more than 100 million y of geological history, the TEX_{86}–SST relationship is strictly a correlation among environmental data. The precise cause of the global correlation and observed deviations within this correlation dataset remain poorly understood (20). Sedimentary GDGTs likely originate from a variety of GDGT-producing organisms, all of which are members of the archaeal domain. Planktonic Thaumarchaeota are considered to be a major source of sedimentary GDGTs, but their populations are often most abundant in subsurface waters, near the base of the photic zone, leaving unknown the causative factor driving the correlations between sedimentary GDGT composition and growth temperature (likely subsurface) (20).

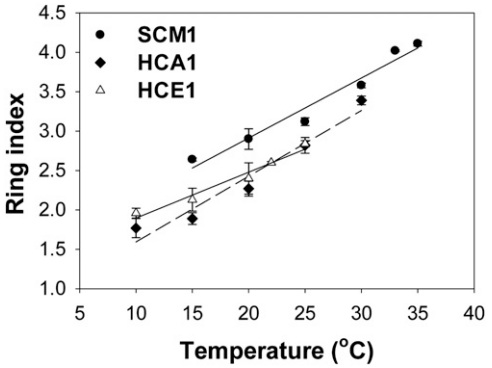

Fig. 3. Correlations of ring index values with growth temperatures of strains SCM1 (15–35 °C), HCA1 (10–30 °C), and HCE1 (10–25 °C). The linear regression lines of SCM1 (solid line), HCA1 (dashed line), and HCE1 (solid line) are $y = 0.076x + 1.40$ ($r^2 = 0.96$), $y = 0.082x + 0.77$ ($r^2 = 0.94$), and $y = 0.058x + 1.31$ ($r^2 = 0.95$), respectively. Error bars represent the SD of data from triplicate cultures (some error bars are too small to be visible in the figure).

Likewise, there is also some contribution from pelagic Euryarchaeota and sediment-dwelling Archaea (42, 43).

Before the availability of pure cultures, mesocosms for North Sea water preincubated at high (27 °C) and low (13 °C) temperatures were used to test the validity of the TEX_{86} proxy (33). The lipid composition was determined following shifts in incubation temperature. Incubations of the high-temperature mesocosm (preincubated at 27 °C) between 10 °C and 35 °C generated TEX_{86} values having the same slope as, but different intercepts from, the global calibration. Even more surprisingly, no linear dependence of growth temperature vs. TEX_{86} values could be found for the low-temperature mesocosm (preincubated at 13 °C) when incubated at the other temperatures (5–35 °C). Instead, a plot of TEX_{86} vs. temperature had a concave down shape (33). However, when all data were combined, the nonlinearity was less apparent (33).

Our use of pure cultures of marine AOA allowed us to independently examine the influence of growth temperature and O_2 on TEX_{86}, and variation in response among different AOA strains. Notably, despite the close phylogenetic relationships, all four marine AOA isolates differed markedly in their TEX_{86} values at the same growth temperature, and strains SCM1, HCA1, and HCE1 exhibited distinctly different temperature–TEX_{86} relationships. The tropical (strain SCM1) and temperate (strains HCA1 and HCE1) marine AOA isolates were initially enriched at 28 °C and 15 °C, respectively (2, 12), temperatures comparable to those (27 °C and 13 °C) applied in the mesocosm study (33). Interestingly, the linear and curved temperature–TEX_{86} trends for strains SCM1, HCA1, and HCE1 are very similar to those observed in the high- and low-temperature mesocosms, respectively (33). The large offsets between TEX_{86}-inferred temperatures and growth temperatures of these isolates (up to 12 °C) are consistent with the mesocosm experiments. The TEX_{86} variation among strains at the same growth temperature suggests this index is reporting both variation in SST and variation in biosynthetic response of distinct AOA ecotypes. In addition, the different temperature optima of our AOA isolates suggest that temperature may select for ecotypes having significantly different temperature–TEX_{86} relationships.

Significant increase in the relative abundance of crenarchaeol with increasing growth temperature was observed with all examined AOA isolates (strains SCM1, HCA1, and HCE1). This suggests the preferential synthesis of crenarchaeol relative to GDGT-1–3 and cren′ could be a common feature for marine AOA in warmer environments, as suggested by the 40 °C temperature optimum of crenarchaeol synthesis (20, 44). Therefore, the ring index equation may be a more suitable proxy for temperature than the TEX_{86} equation. Indeed, although no linear dependence of growth temperature and TEX_{86} values was found for some isolates, there was a linear relationship between ring index values and growth temperatures for all of the marine AOA examined in this study. Notably, the temperate isolates (HCA1 and HCE1), having a growth optimum near 25 °C, displayed a similar degree of cyclization of total GDGTs at a given temperature. In contrast, strain SCM1 produced a membrane with a higher ring index than temperate isolates at all temperatures, possibly related to its adaptation to higher-temperature environments. However, further studies are needed to more fully evaluate the utility of ring index values as a complementary temperature proxy.

Alternative factors known to influence membrane composition of archaea include pH and salinity. The GDGT composition of the cultured thermophilic AOA *Nitrosocaldus yellowstonii* and members of Crenarchaeota vary with pH (20, 45–47). However, for the highly buffered ocean, pH variability is relatively small, and thus would not be expected to significantly bias reconstructed SST. In addition, although salinity has been shown to exert substantial control on the lipid composition of halophilic archaea (48), no significant variation of GDGT distributions was found in a marine mesocosm study where salinity was varied (33). In contrast, the influence of O_2 concentration on lipid composition is relatively unexplored. Thus, the striking response of the marine AOA isolates to reduced O_2 was surprising, demonstrating an increase in TEX_{86}-derived temperatures of up to 21 °C by varying O_2 concentration alone.

O_2 concentrations are known to span a wide range of values with depth in the ocean and in sediment. Suboxia and anoxia prevail in some modern enclosed basins and in restricted waterways present early in Earth history such as the Atlantic Ocean during the Oceanic Anoxic Events (OAE) of the Cretaceous and Jurassic periods (49). Presently, the ocean is also home to several large OMZs where subsurface waters experience varying degrees of suboxia and anoxia. Thus, our observation of a major controlling influence of O_2 on TEX_{86} values is important for interpretation of environments and sedimentary records influenced by low O_2 or anoxia. Notably, anomalously warm TEX_{86} patterns of SPM samples have been reported over a wide range of suboxic settings, such as in the permanent OMZ of the Arabian Sea and the Eastern Tropical North Pacific Ocean, and seasonally O_2-deficient regions in coastal upwelling areas (27, 28, 50). In addition, TEX_{86} values of sediment recovered from the summit of the Murray Ridge seamount that extends into the OMZ of the Arabian Sea were higher than those of sediment recovered from adjacent deeper locations well below the OMZ, and the reconstructed TEX_{86} temperatures from sediment cores within the OMZ were more than 5 °C higher than the mean annual SST (51).

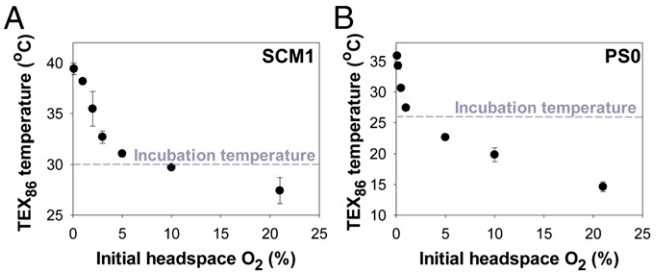

Fig. 4. Reconstructed TEX_{86} temperatures for the total cellular lipids of strains SCM1 (*A*) and PS0 (*B*) showing the exponential TEX_{86}-derived temperature increase from 21% O_2 to 0.1% O_2. Dashed lines represent the constant incubation temperature of strains SCM1 (*A*) and PS0 (*B*) at 30 °C and 26 °C, respectively. Error bars represent the SD of the mean of triplicate cultures.

Although surface waters are not O_2-deficient in these areas, the AOA are of higher abundance in the oxycline and upper OMZ where waters can be oxygen-deficient (9, 10). The AOA living under O_2 limitation would likely be the major contributor to the sedimentary GDGTs collected within the Arabian Sea OMZ (51). Elevated TEX_{86} values were mainly the result of the relative increase in GDGT-2 that we have now shown to increase under low O_2 concentrations with pure cultures of marine AOA (25, 27, 28). Thus, our study clearly implicates a lipid biosynthetic response as a causative factor in producing anomalously high TEX_{86} values within low-oxygen environments. In addition, if reduced O_2 concentrations select for a different marine archaeal community, then an altered species composition could also influence the composition of GDGTs preserved in the sediments. However, resolving the relative importance of adaptation vs. selection on the TEX_{86} record in response to "greenhouse" climates will require a more complete understanding of thaumarchaeal ecophysiology.

Our laboratory findings may also provide an explanation for some unexpected TEX_{86} sedimentary records. The Jurassic and Cretaceous Periods are known as relatively warm intervals in Earth's history. One consequence of warmer water is lower DO, because O_2 is less soluble in warm water than in cold water. TEX_{86}-derived temperature records of this time period routinely exceed modern temperatures at equivalent latitudes (22, 29, 52–54). Our results suggest decreased DO concentrations of warm ancient seawater would raise reconstructed temperatures to values somewhat higher than the actual SST. During particular intervals of Earth's history, such as the many OAEs and Paleocene/Eocene thermal maximum (PETM), widespread dysoxic or even anoxic conditions impinged on the photic zone, as indicated by a sedimentary biomarker (isorenieratane) for photic zone anoxia (31, 49, 53, 55, 56). Although some increase in temperature during OAEs and the PETM is consistent with paleoclimate model simulations and planktonic foraminiferal $\delta^{18}O$-based SST reconstructions, TEX_{86} values (as high as 0.95) and TEX_{86}-derived temperatures (up to 43 °C) observed during these low-oxygen events seem anomalously high (31, 53–58). However, because $\delta^{18}O$-based temperature estimates are not available throughout the black shales of an OAE, there is no independent validation of the exceptionally warm TEX_{86}-inferred temperatures for these climate periods (31, 59, 60).

Excursions in O_2 concentration are also associated with short historic periods of pronounced cooling (53, 54, 61). For example, the TEX_{86} paleotemperature proxy suggests a cooling of up to 12 °C during the Plenus Cold Event (PCE) of OAE-2 (54). However, the PCE is also marked by a drop in isorenieratane concentrations in the sedimentary record, indicative of reoxygenation of a previously anoxic photic zone (53). Because the steep decrease in TEX_{86} values within OAEs is difficult to explain with a drastic drop of SSTs only, reoxygenation would offer an explanation for large swings in TEX_{86} values observed during these events. Thus, together our data now implicate DO as an additional causative factor of anomalously high or low TEX_{86} values and inferred temperatures.

We recognize that more experiments with AOA strains representing a broader range of ecotypes are necessary to further explore environmental influences on GDGT composition and how these factors relate to physiology. There also remains the question of the biophysical significance of thaumarchaeal membrane compositional changes associated with reduced O_2 concentration. It has been suggested that an increase in cyclopentane rings reduces proton permeability as a result of denser membrane packing (19, 62). This adaptive response may allow AOA to cope with the energy stress of low-O_2 environments, such as the boundary of the OMZs in today's oceans and during past periods of low O_2 availability, such as the OAE of the mid-Cretaceous. However, apart from the questions of physiological significance highlighted by these studies, the available data do offer an argument in favor of viewing the global calibration datasets of TEX_{86} index as a compilation of local calibrations (20) and point to the need to reevaluate inferences of paleoclimate from geologic records where conditions differ significantly from the modern and from unique local environments such as those underlying OMZs.

Finally, in addition to the significance of our observations for reinterpreting past climates and oceanic conditions, the adaptive response of these AOA may have relevance to predicting the response of oceanic populations affected by climate change. Predicted warming, deoxygenation, and acidification of the global ocean will certainly have an impact on major biogeochemical systems (63–65). Thus, better resolving the physiological response of marine AOA to these changes is of global significance. Phenotypic plasticity that enhances the adaptive capacity of AOA may mitigate some of these responses with important implications for both adaptation to and reconstruction of change in present and past marine environments, respectively.

Methods

Culture Maintenance and Experimental Setup. All materials and methods for marine AOA pure culture maintenance and temperature and O_2 growth experiments are described in detail in *SI Appendix, Materials and Methods*.

Lipid Extraction and Analysis. Lipids were extracted from 0.22-μm Durapore membrane filters (Millipore Co.) containing early stationary phase cells and analyzed using atmospheric pressure chemical ionization on an Agilent 1100 Series liquid chromatograph coupled to an Agilent ion trap mass spectrometer. For details, see *SI Appendix, Materials and Methods*.

Calculation of TEX_{86} Index, TEX_{86}-Derived Temperature, and Ring Index. The TEX_{86} values were calculated based on the relative abundances of GDGT-1, GDGT-2, GDGT-3, and Cren′ using the respective peak areas (21):

$$TEX_{86} = \frac{[GDGT-2]+[GDGT-3]+[Cren']}{[GDGT-1]+[GDGT-2]+[GDGT-3]+[Cren']}. \quad [4]$$

The reconstructed TEX_{86} temperatures were calculated on the basis of the core-top linear calibration of Kim et al. (39):

$$SST = -10.78 + 56.2 \times TEX_{86} \left(r^2 = 0.94\right). \quad [5]$$

The ring index was calculated according to Pearson et al. (40):

$$\text{Ring index} = \frac{[\text{GDGT}-1]+2\times[GDGT-2]+3\times[GDGT-3]+5\times[Cren+Cren']}{[GDGT-0]+[GDGT-1]+[GDGT-2]+[GDGT-3]+[Cren+Cren']}. \quad [6]$$

ACKNOWLEDGMENTS. We thank Kelley Meinhardt, Julia Kobelt, Frederick Von Netzer, Angie Boysen, and David French for technical assistance, and Willm Martens-Habbena, Shady Amin, Birte Meyer, and Katherine Heal for invaluable discussions. This work was funded by National Science Foundation Grants MCB-0604448 and MCB-0920741 (to D.A.S.) and Dimensions of Biodiversity Program Grants OCE-1046017 (to D.A.S., E.V.A., A.H.D., J.W.M., and A.E.I.) and OCE-1029281 and OCE-1205232 (to A.E.I.).

1. Brochier-Armanet C, Boussau B, Gribaldo S, Forterre P (2008) Mesophilic Crenarchaeota: Proposal for a third archaeal phylum, the Thaumarchaeota. *Nat Rev Microbiol* 6(3):245–252.
2. Könneke M, et al. (2005) Isolation of an autotrophic ammonia-oxidizing marine archaeon. *Nature* 437(7058):543–546.
3. Karner MB, DeLong EF, Karl DM (2001) Archaeal dominance in the mesopelagic zone of the Pacific Ocean. *Nature* 409(6819):507–510.
4. Francis CA, Roberts KJ, Beman JM, Santoro AE, Oakley BB (2005) Ubiquity and diversity of ammonia-oxidizing archaea in water columns and sediments of the ocean. *Proc Natl Acad Sci USA* 102(41):14683–14688.
5. Beman JM, Popp BN, Alford SE (2012) Quantification of ammonia oxidation rates and ammonia-oxidizing archaea and bacteria at high resolution in the Gulf of California and eastern tropical North Pacific Ocean. *Limnol Oceanogr* 57(3):711–726.
6. Horak REA, et al. (2013) Ammonia oxidation kinetics and temperature sensitivity of a natural marine community dominated by Archaea. *ISME J* 7(10):2023–2033.
7. Martens-Habbena W, et al. (2015) The production of nitric oxide by marine ammonia-oxidizing archaea and inhibition of archaeal ammonia oxidation by a nitric oxide scavenger. *Environ Microbiol* 17(7):2261–2274.

8. Yan J, et al. (2012) Mimicking the oxygen minimum zones: Stimulating interaction of aerobic archaeal and anaerobic bacterial ammonia oxidizers in a laboratory-scale model system. *Environ Microbiol* 14(12):3146–3158.
9. Lam P, et al. (2009) Revising the nitrogen cycle in the Peruvian oxygen minimum zone. *Proc Natl Acad Sci USA* 106(12):4752–4757.
10. Hawley AK, Brewer HM, Norbeck AD, Paša-Tolić L, Hallam SJ (2014) Metaproteomics reveals differential modes of metabolic coupling among ubiquitous oxygen minimum zone microbes. *Proc Natl Acad Sci USA* 111(31):11395–11400.
11. Santoro AE, Buchwald C, McIlvin MR, Casciotti KL (2011) Isotopic signature of N_2O produced by marine ammonia-oxidizing archaea. *Science* 333(6047):1282–1285.
12. Qin W, et al. (2014) Marine ammonia-oxidizing archaeal isolates display obligate mixotrophy and wide ecotypic variation. *Proc Natl Acad Sci USA* 111(34):12504–12509.
13. Martens-Habbena W, Berube PM, Urakawa H, de la Torre JR, Stahl DA (2009) Ammonia oxidation kinetics determine niche separation of nitrifying Archaea and Bacteria. *Nature* 461(7266):976–979.
14. Amin SA, et al. (2013) Copper requirements of the ammonia-oxidizing archaeon *Nitrosopumilus maritimus* SCM1 and implications for nitrification in the marine environment. *Limnol Oceanogr* 58(6):2037–2045.
15. Könneke M, et al. (2014) Ammonia-oxidizing archaea use the most energy-efficient aerobic pathway for CO_2 fixation. *Proc Natl Acad Sci USA* 111(22):8239–8244.
16. Walker CB, et al. (2010) *Nitrosopumilus maritimus* genome reveals unique mechanisms for nitrification and autotrophy in globally distributed marine crenarchaea. *Proc Natl Acad Sci USA* 107(19):8818–8823.
17. Elling FJ, et al. (2014) Effects of growth phase on the membrane lipid composition of the thaumarchaeon *Nitrosopumilus maritimus* and their implications for archaeal lipid distributions in the marine environment. *Geochim Cosmochim Acta* 141: 579–597.
18. van de Vossenberg JLCM, Driessen AJM, Konings WN (1998) The essence of being extremophilic: The role of the unique archaeal membrane lipids. *Extremophiles* 2(3): 163–170.
19. Valentine DL (2007) Adaptations to energy stress dictate the ecology and evolution of the Archaea. *Nat Rev Microbiol* 5(4):316–323.
20. Pearson A, Ingalls AE (2013) Assessing the use of archaeal lipids as marine environmental proxies. *Annu Rev Earth Planet Sci* 41:359–384.
21. Schouten S, Hopmans EC, Schefuß E, Damsté JSS (2002) Distributional variations in marine crenarchaeotal membrane lipids: A new tool for reconstructing ancient sea water temperatures? *Earth Planet Sci Lett* 204(1–2):265–274.
22. Jenkyns HC, Schouten-Huibers L, Schouten S, Damsté JSS (2012) Warm Middle Jurassic-Early Cretaceous high-latitude sea-surface temperatures from the Southern Ocean. *Clim Past* 8(1):215–226.
23. Trommer G, et al. (2009) Distribution of Crenarchaeota tetraether membrane lipids in surface sediments from the Red Sea. *Org Geochem* 40(6):724–731.
24. Shevenell AE, Ingalls AE, Domack EW, Kelly C (2011) Holocene Southern Ocean surface temperature variability west of the Antarctic Peninsula. *Nature* 470(7333): 250–254.
25. Kim J-H, et al. (2015) Influence of deep-water derived isoprenoid tetraether lipids on the TEX_{86} paleothermometer in the Mediterranean Sea. *Geochim Cosmochim Acta* 150(0):125–141.
26. Ingalls AE, et al. (2006) Quantifying archaeal community autotrophy in the mesopelagic ocean using natural radiocarbon. *Proc Natl Acad Sci USA* 103(17):6442–6447.
27. Xie ST, Liu XL, Schubotz F, Wakeham SG, Hinrichs KU (2014) Distribution of glycerol ether lipids in the oxygen minimum zone of the Eastern Tropical North Pacific Ocean. *Org Geochem* 71:60–71.
28. Basse A, et al. (2014) Distribution of intact and core tetraether lipids in water column profiles of suspended particulate matter off Cape Blanc, NW Africa. *Org Geochem* 72:1–13.
29. Schouten S, et al. (2003) Extremely high sea-surface temperatures at low latitudes during the middle Cretaceous as revealed by archaeal membrane lipids. *Geology* 31(12):1069–1072.
30. Kim JH, et al. (2010) New indices and calibrations derived from the distribution of crenarchaeal isoprenoid tetraether lipids: Implications for past sea surface temperature reconstructions. *Geochim Cosmochim Acta* 74(16):4639–4654.
31. Sluijs A, et al.; Expedition 302 Scientists (2006) Subtropical Arctic Ocean temperatures during the Palaeocene/Eocene thermal maximum. *Nature* 441(7093):610–613.
32. Wuchter C, Schouten S, Wakeham SG, Damsté JSS (2005) Temporal and spatial variation in tetraether membrane lipids of marine Crenarchaeota in particulate organic matter: Implications for TEX_{86} paleothermometry. *Paleoceanography* 20(3), 10.1029/2004PA001110.
33. Wuchter C, Schouten S, Coolen MJL, Damsté JSS (2004) Temperature-dependent variation in the distribution of tetraether membrane lipids of marine Crenarchaeota: Implications for TEX_{86} paleothermometry. *Paleoceanography* 19(4), 10.1029/2004PA001041.
34. Hopmans EC, Schouten S, Pancost RD, van der Meer MTJ, Sinninghe Damsté JS (2000) Analysis of intact tetraether lipids in archaeal cell material and sediments by high performance liquid chromatography/atmospheric pressure chemical ionization mass spectrometry. *Rapid Commun Mass Spectrom* 14(7):585–589.
35. Huguet C, et al. (2010) Changes in intact membrane lipid content of archaeal cells as an indication of metabolic status. *Org Geochem* 41(9):930–934.
36. Hedrick DB, Guckert JB, White DC (1991) Archaebacterial ether lipid diversity analyzed by supercritical fluid chromatography: Integration with a bacterial lipid protocol. *J Lipid Res* 32(4):659–666.
37. Ferrante G, Ekiel I, Patel GB, Sprott GD (1988) Structure of the major polar lipids isolated from the aceticlastic methanogen, *Methanothrix concilii* Gp6. *Biochim Biophys Acta* 963(2):162–172.
38. Langwort TA, Mayberry WR, Smith PF (1974) Long-chain glycerol diether and polyol dialkyl glycerol triether lipids of *Sulfolobus acidocaldarius*. *J Bacteriol* 119(1):106–116.
39. Kim JH, Schouten S, Hopmans EC, Donner B, Damste JSS (2008) Global sediment core-top calibration of the TEX_{86} paleothermometer in the ocean. *Geochim Cosmochim Acta* 72(4):1154–1173.
40. Pearson A, et al. (2004) Nonmarine crenarchaeol in Nevada hot springs. *Appl Environ Microbiol* 70(9):5229–5237.
41. Stewart FJ, Ulloa O, DeLong EF (2012) Microbial metatranscriptomics in a permanent marine oxygen minimum zone. *Environ Microbiol* 14(1):23–40.
42. Lipp JS, Morono Y, Inagaki F, Hinrichs KU (2008) Significant contribution of Archaea to extant biomass in marine subsurface sediments. *Nature* 454(7207):991–994.
43. Lincoln SA, et al. (2014) Planktonic Euryarchaeota are a significant source of archaeal tetraether lipids in the ocean. *Proc Natl Acad Sci USA* 111(27):9858–9863.
44. Zhang CL, Pearson A, Li YL, Mills G, Wiegel J (2006) Thermophilic temperature optimum for crenarchaeol synthesis and its implication for archaeal evolution. *Appl Environ Microbiol* 72(6):4419–4422.
45. de la Torre JR, Walker CB, Ingalls AE, Könneke M, Stahl DA (2008) Cultivation of a thermophilic ammonia oxidizing archaeon synthesizing crenarchaeol. *Environ Microbiol* 10(3):810–818.
46. Pearson A, et al. (2008) Factors controlling the distribution of archaeal tetraethers in terrestrial hot springs. *Appl Environ Microbiol* 74(11):3523–3532.
47. Boyd ES, et al. (2011) Temperature and pH controls on glycerol dibiphytanyl glycerol tetraether lipid composition in the hyperthermophilic crenarchaeon *Acidilobus sulfurireducens*. *Extremophiles* 15(1):59–65.
48. Dawson KS, Freeman KH, Macalady JL (2012) Molecular characterization of core lipids from halophilic archaea grown under different salinity conditions. *Org Geochem* 48: 1–8.
49. Meyer KM, Kump LR (2008) Oceanic euxinia in Earth history: Causes and consequences. *Annu Rev Earth Planet Sci* 36:251–288.
50. Schouten S, et al. (2012) Intact polar and core glycerol dibiphytanyl glycerol tetraether lipids in the Arabian Sea oxygen minimum zone: I. Selective preservation and degradation in the water column and consequences for the TEX_{86}. *Geochim Cosmochim Acta* 98:228–243.
51. Lengger SK, et al. (2012) Intact polar and core glycerol dibiphytanyl glycerol tetraether lipids in the Arabian Sea oxygen minimum zone. Part II: Selective preservation and degradation in sediments and consequences for the TEX_{86}. *Geochim Cosmochim Acta* 98:244–258.
52. Littler K, Robinson SA, Bown PR, Nederbragt AJ, Pancost RD (2011) High sea-surface temperatures during the Early Cretaceous Epoch. *Nat Geosci* 4(3):169–172.
53. van Bentum EC, Reichart GJ, Forster A, Damsté JSS (2012) Latitudinal differences in the amplitude of the OAE-2 carbon isotopic excursion: pCO_2 and paleo productivity. *Biogeosciences* 9(2):717–731.
54. Damsté JSS, van Bentum EC, Reichart GJ, Pross J, Schouten S (2010) A CO_2 decrease-driven cooling and increased latitudinal temperature gradient during the mid-Cretaceous Oceanic Anoxic Event 2. *Earth Planet Sci Lett* 293(1-2):97–103.
55. Schoon PL, Heilmann-Clausen C, Schultz BP, Sinninghe Damsté JS, Schouten S (2014) Warming and environmental changes in the eastern North Sea Basin during the Palaeocene-Eocene Thermal Maximum as revealed by biomarker lipids. *Org Geochem* 78(0):79–88.
56. Sluijs A, et al. (2014) Warming, euxinia and sea level rise during the Paleocene-Eocene Thermal Maximum on the Gulf Coastal Plain: Implications for ocean oxygenation and nutrient cycling. *Clim Past* 10(4):1421–1439.
57. van Helmond NAGM, et al. (2014) A perturbed hydrological cycle during Oceanic Anoxic Event 2. *Geology* 42(2):123–126.
58. Zachos JC, et al. (2006) Extreme warming of mid-latitude coastal ocean during the Paleocene-Eocene Thermal Maximum: Inferences from TEX_{86} and isotope data. *Geology* 34(9):737–740.
59. Erbacher J, Huber BT, Norris RD, Markey M (2001) Increased thermohaline stratification as a possible cause for an ocean anoxic event in the Cretaceous period. *Nature* 409(6818):325–327.
60. Wagner T, et al. (2008) Rapid warming and salinity changes of Cretaceous surface waters in the subtropical North Atlantic. *Geology* 36(3):203–206.
61. Forster A, Schouten S, Moriya K, Wilson PA, Damsté JSS (2007) Tropical warming and intermittent cooling during the Cenomanian/Turonian oceanic anoxic event 2: Sea surface temperature records from the equatorial Atlantic. *Paleoceanography* 22(1), 10.1029/2006PA001349.
62. Gabriel JL, Chong PLG (2000) Molecular modeling of archaebacterial bipolar tetraether lipid membranes. *Chem Phys Lipids* 105(2):193–200.
63. Matear RJ, Hirst AC (2003) Long-term changes in dissolved oxygen concentrations in the ocean caused by protracted global warming. *Glob Biogeochem Cycles* 17(4), 10.1029/2002GB001997.
64. Orr JC, et al. (2005) Anthropogenic ocean acidification over the twenty-first century and its impact on calcifying organisms. *Nature* 437(7059):681–686.
65. Meehl GA, et al. (2005) How much more global warming and sea level rise? *Science* 307(5716):1769–1772.